Enhanced performance of ultra-thin $Cu(In,Ga)Se_2$ solar cells deposited at low process temperature

G. Yin [a], V. Brackmann [b], V. Hoffmann [b], M. Schmid [a]

[a]Helmholtz-Zentrum Berlin für Materialien und Energie, Nanooptical Concepts for PV, 14109 Berlin, Germany

[b]IFW Dresden, Institut für Komplexe Materialien, 270116 Dresden, Germany

Corresponding author: guanchao.yin@helmholtz-berlin.de (G. Yin)

Tel: +49 30 806243721, fax: +49 30 806243199

Abstract: To investigate the process temperature on the growth of ultra-thin (≤ 500 nm) $Cu(In,Ga)Se_2$ (CIGSe) absorbers and the corresponding performance of solar cells, the process temperature was set to 610 °C and 440 °C, respectively. It was found that the low process temperature (440 °C) could reduce the inter-diffusion of Ga-In and thus result in a higher back [Ga]/([Ga]+[In]) ([Ga]/[III]) grading than at the temperature of 610 °C. The higher back [Ga]/[III] grading at 440 °C was evidenced to both electrically and optically contribute to the efficiency enhancement of the solar cells in contrast to the lower back [Ga]/[III] grading at 610 °C. It was also implied that the high back [Ga]/[III] grading was beneficial to the collection of carriers generated from the back-reflected light.

Keywords: CIGSe, low process temperature, ultra-thin, back Ga grading

1. Introduction

Reducing the absorber thickness is critical to realizing the reduction of material consumption (e.g Indium and Gallium) and resulting cost of $Cu(In,Ga)Se_2$ (CIGSe) solar cells [1, 2]. However, high efficiencies are only achieved with absorbers thicker than 1 μm [3-4]. Further reducing the absorber thickness to 0.5 μm has been experimentally shown to considerably reduce the efficiency. The dominating reason behind

the poor performance of ultra-thin solar cells (with absorber thickness below 0.5 µm) is the substantial drop of short current density (J_{sc}) [3-5], which is assumed to mainly originate from the incomplete absorption of the incident solar spectrum and the strong carrier recombination at the back contact (back recombination).

Concerning the back recombination, the risk is much higher for ultra-thin solar cells due to the reduced distance of electrons to the back contact [6]. It is extensively reported that an increasing [Ga]/([Ga]+[In]) ratio ([Ga]/[III]) towards the back contact (the back Ga grading) can serve as an electron back reflector by increasing the conduction band (CB) and thus reduce the carrier recombination [6-11]. Furthermore, Vermang [12] introduced a back passivation structure by depositing an Al_2O_3 film on the nano-sphere coated Mo substrate, which decreased the back recombination as well. In spite of this, there has been no experimental comparison of the efficacy of back recombination passivation between a higher back Ga grading and a back passivation structure. In the 3-stage co-evaporation processes [13], lowering process temperature (substrate temperature) was proved to be able to reduce the inter-diffusion of Ga-In [14, 15] and therefore provides the possibility to create a higher back Ga grading by engineering the deposition sequence of Ga-Se precursor and In-Se. At the same time, the low process temperature can enable the preparation of CIGSe solar cells on flexible polymer substrates [16, 17], thus offering a potential to further reduce the manufacturing cost and widen the applications of the solar cells.

However, high-quality CIGSe absorbers are normally deposited above 500 °C. How the low process temperature affects the ultra-thin absorbers and resulting performances of CIGSe solar cells is still unknown in detail y. To identify this, we will investigate solar cells deposited at low process temperature and compare the results to those at high process temperature.

2. Experimental

CIGSe absorbers were fabricated on Mo substrates by the 3-stage co-evaporation process. To create a high intentional back Ga grading, the Ga-Se precursor was deposited before the In-Se at 410 °C during the 1st stage of the 3 stages of the evaporation. Cu-Se and In-Ga-Se precursors were evaporated at the substrate temperature T_S during the 2nd and 3rd stage, respectively. T_S is higher than the temperature of 410 °C in the 1st stage and is defined as the process temperature. After reaching the [Cu]/([Ga]+[In]) ratio ([Cu]/[III]) of 1.06 at the end of the 2nd stage, the process transitioned to the 3rd stage and terminated at the [Cu]/[III] ratio of around 0.85-0.9. Laser light scattering (LLS) was used for the in-situ control of the process [18]. The composition ratios mentioned above are the estimated values from LLS signal. To compare the influence of T_S on the absorbers, T_S was set to 610°C and 440°C. For evaluating the absorption coefficient α of the absorbers, a reference sample was deposited on glass substrate at each temperature.

The substrate used was soda lime glass (SLG) with a thickness of 2 mm. The 800 nm thick Mo layer was sputtered onto the SLG substrate with a sheet resistance 0.8 Ω/□ for back contact. For the device completion, a 100 nm thick CdS layer was grown by a standard chemical bath deposition (CBD) process after the CIGSe deposition. The CBD process was performed in a solution with 1.1 M ammonia, 0.14 M Thiourea and 0.002M Cadmium Acetate. A sputtered 130 nm i-ZnO and a 240 nm Al doped ZnO (AZO) layer followed the CdS. The Ni/Al front contact grid was evaporated through a shadow mask with a total thickness of 2500 nm. Finally, 0.5 cm^2 solar cells were mechanically scribed including the area of the front contact grid.

For characterization of the absorber morphology, scanning electron microscopy (SEM) was used. The element composition of the absorbers was measured by X-ray fluorescence analysis (XRF). The overall [Ga]/[III] and [Cu]/[III] ratio are 0.4±0.01 and 0.86±0.01, respectively. The thickness of absorbers was evaluated by both XRF and optical simulation of the CIGSe samples on glass substrates [19]. The

thickness in both cases is 460±5nm. The phase structure was characterized by X-ray diffraction (XRD). Glow discharge optical emission spectrometry (GDOES) was used to evaluate the [Ga]/[III] depth profile across the CIGSe absorber. The GDOES measurement was performed by a spectrometer (GDA 650 from Spectruma) with 2,5 mm anode and Ar discharge gas [20, 21]. The I-V curve was measured under standard test conditions (AM 1.5; 100mW/cm^2; 25°C) by a home-made system with a sun-simulator (WXS-140S-SUPER from WACOM), which consists of both a Xenon and a Halogen lamp. The AM1.5 condition is calibrated by a certified crystalline Si solar cell from the Fraunhofer Institute for Solar Energy Systems (ISE). The external quantum efficiency (EQE) was measured with a two-source illumination system of a Xenon and a Halogen Lamp, using a calibrated a Si and a Ge diode as references.

3. Results and discussion

3.1 Morphology and [Ga]/[III] depth profile

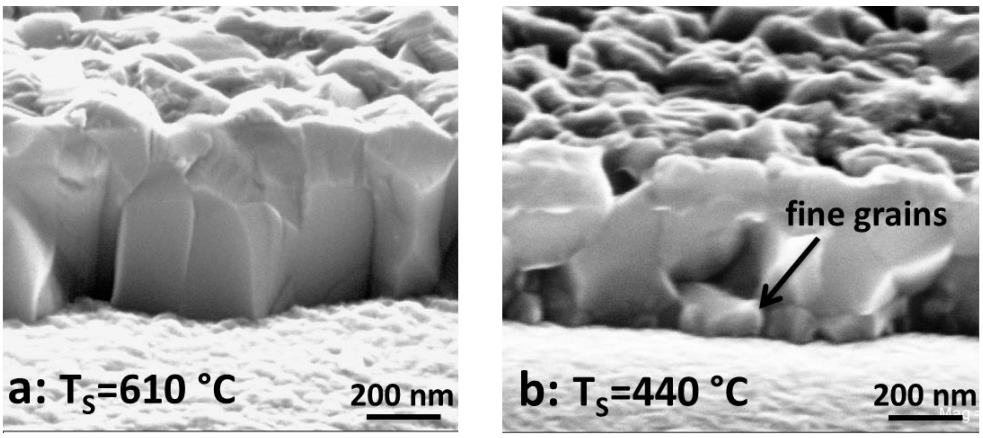

Fig. 1. Cross sections of the CIGSe layers on Mo substrate at process temperatures of (a) T_S = 610 °C, (b) T_S = 440 °C

Fig. 1 displays the morphology of CIGSe layers in cross section at different process temperatures T_S. During the 3-stage process deposition, the maximum temperature T_S dominates the growth of the absorbers, which can be also observed in Fig. 1. At the high temperature T_S = 610 °C, the grains are

closely packed and extend through the entire thickness. At T_S = 440 °C, there still exist large grains but with fine grains near the Mo back contact, which was correlated to high [Ga]/[III] CIGSe phases by Kaufmann [15]. Fig. 2(a) shows the (112) XRD diffraction peaks of the absorbers at the two process temperatures. In contrast to the single and sharp peak for the absorber deposited at T_S = 610 °C, the (112) diffraction peak evolves into a broad double-peak when the process temperature T_S drops to 440 °C. Besides, the two sub-peaks locate at each side of the single peak corresponding to T_S = 610 °C. Because of a larger atomic radius of In than Ga, as the [Ga]/[III] ratio increases , the peak position is evolving from CISe with the lowest 2 theta value to CGSe with the highest. Since the two absorbers have the same overall [Ga]/[III] ratio , the double-peak at T_S = 440 °C indicates a reduced inter-diffusion of Ga-In. Combining the fact of the intentional deposition of the Ga-Se precursor before In-Se during the 1st stage of the 3-stage deposition, the higher [Ga]/[III] CIGSe phases near the back contact are expected. To further determine the [Ga]/[III] depth profiles across the absorbers, GDOES was performed on the absorbers and results are shown in Fig. 2(b). At T_S = 610 °C, the absorber shows a relatively flat Ga depth distribution, while at T_S = 440 °C the Ga distribution has a distinct grading both towards the surface and back side, but especially towards the back side. Conclusively, GDOES results further confirm that the intentional back Ga grading by the deposition of the Ga-Se before In-Se in the 1st stage is much flattened at T_S = 610 °C and largely preserved at T_S = 440 °C. The 3-stage deposition process can normally result in a double-graded [Ga]/[III] profile with a higher [Ga]/[III] ratio towards both the back and front of the absorber, and a typical notch point with the lowest [Ga]/[III] ratio in between. Because of the linear dependence of the bandgap of CIGSe phases on the [Ga]/[III] ratio from 1.01 eV (CISe) to 1.67 (CGSe), there exist a minimum bandgap ($E_{g,min}$) at the notch point. From Fig. 2(b), it can be concluded that $E_{g,min}$ for the absorber at T_S = 440 °C is lower than that at T_S = 610 °C.

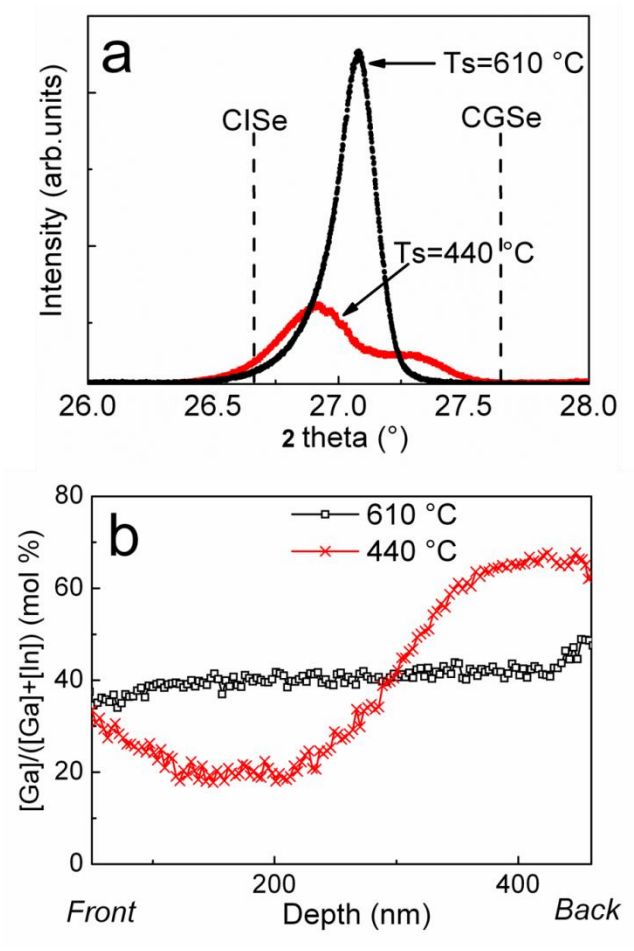

Fig. 2. (a) (112) XRD diffraction peaks and (b) the corresponding [Ga]/[III] depth profiles evaluated by GDOES at both temperatures.

3.2 Device performance

Table 1

I-V device performances under standard AM 1.5 illumination (average results from 6 solar cells at each process temperature)

T_S	V_{oc} (mV)	J_{sc} (mA/cm^2)	FF (%)	η (%)
610 °C	624	22.2	64.4	9.0

440 °C	591	26.6	67.5	10.6

Table 1 compares the I-V performances of the solar cells at two different process temperatures. As the temperature is lowered to T_S = 440 °C, the V_{oc} decreases moderately by 5.3%, which can be mainly interpreted due to the lower $E_{g,min}$ [22] as evaluated above, but the substantial increase of J_{sc} and maintained FF contribute to the considerable net enhancement (relatively 17.8%) in efficiency. Kaufmann [15] conducted similar experiments for solar cells with an approximate 2-µm thick absorber. However, the η deteriorated severely due to the large drop of V_{oc} and FF even with the increase of J_{sc} at lower process temperature. Generally a higher density of bulk recombination defects is expected and this results in the large drop of V_{oc} and FF at lower process temperature. However, our ultra-thin solar cells exhibit a maintained FF and only relatively moderate drop of V_{oc}. This can be interpreted due to two aspects. Firstly, the width of the space charge region (SCR) is normally about 300-500 nm [23, 24], which is comparable to the thickness of our ultra-thin absorbers. This means most photo-generated carriers are located within the SCR, carrier collection efficiency can be thus kept high even in the case of decreased lifetime of carriers resulting from a high defect density at low process temperature. It was theoretically proved [6] that the performance of the ultra-thin solar cells was tolerant towards the decrease of the lifetime of carriers; secondly, as is confirmed by GDOES in Fig. 2(b), the back Ga grading is much higher for the absorber deposited at T_S = 440 °C than that at T_S = 610 °C. This reduces the back recombination and enhances the carrier collection efficiency for the solar cell at T_S = 440 °C. The improved carrier collection not only enhances the J_{sc}, but also helps FF and V_{oc}.

Fig. 3 displays the EQE curves of the solar cells at the two different temperatures T_S. We can observe an averaged overall improvement in EQE for the solar cells at T_S = 440 °C compared to those at T_S = 610 °C. The results are in accordance with the increase of the J_{sc} shown in Table 1. In the wavelength range below 580nm, the enhancement in EQE, is possibly due to the variation of the thickness of CdS. The

enhancement above the wavelength of 600 nm is attributed to the high back Ga grading for the solar cell deposited at T_S = 440 °C. It accounts for 67% of the enhancement in J_{sc}. In more detail, several factors are assumed to contribute to the broad improvement of EQE above the wavelength of 600 nm. The first one is the reduced back recombination because of the increased back Ga grading, which we analysed above. What is more, a lower $E_{g,min}$ for the absorber at T_S = 440 °C implies a broader absorption spectrum. This can be also reflected by the corresponding EQE, which shows a broader collection wavelength range. To quantitatively prove this, the absorption coefficients α of each absorber on glass substrate were calculated [25] and are illustrated in Fig. 4. It can be observed that the absorber deposited at T_S = 440 °C exhibits absorption ability not only in a broader spectrum range than that at T_S = 610 °C, but also higher beyond 930 nm. This indicates that the [Ga]/[III]depth profile can also influence the absorption coefficient α, which is not only dependent on the overall [Ga]/[III] ratio usually assumed in literature [26, 27]. Since the lower [Ga]/[III] CIGSe phases have higher absorption coefficients and broader absorption spectrum (discovered by our own calculation as well as in literature [26, 27]) , the absorber at T_S = 440 °C, which holds a larger proportion of low [Ga]/[III] phases, shows a higher absorption ability beyond 930 nm and extend absorption ability up to approx. 1200 nm. Therefore, the improved absorption ability at T_S = 440 °C also contributes to an increase of EQE in the wavelength range of 930-1200 nm.

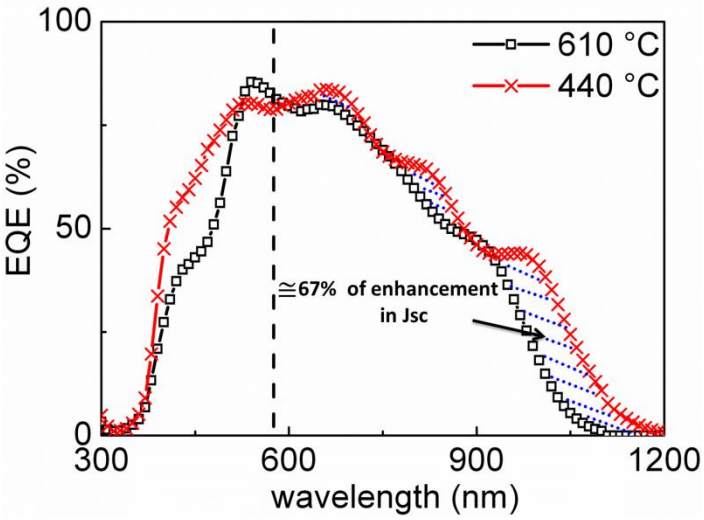

Fig. 3. External quantum efficiency (EQE) of solar cells with absorbers deposited at T_S = 610 °C and T_S = 440 °C, respectively.

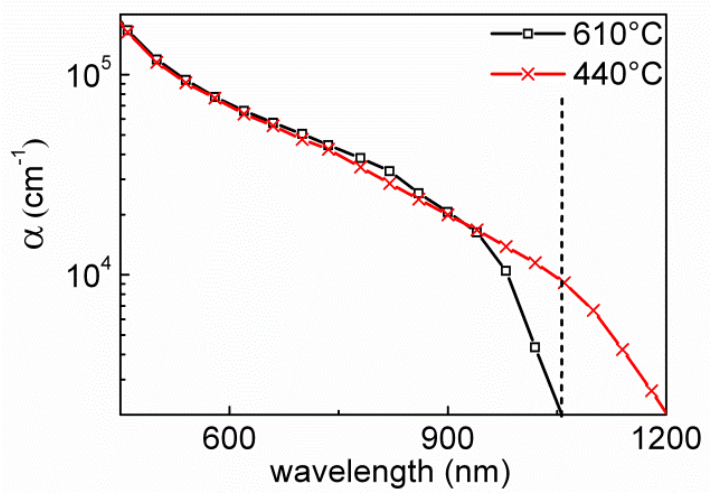

Fig. 4. Calculated absorption coefficient α of reference samples on glass substrate at varied process temperatures of T_S = 610 °C and T_S = 440 °C.

Returning to the benefit of the reduced back recombination resulting from the higher back Ga grading, this has been extensively investigated both experimentally and theoretically [6-11]. It was proved that the high back Ga grading could benefit the performance of solar cells mainly in terms of an improvement of both V_{oc} and J_{sc}[6]. This is also confirmed by our experimental data in Table 1. Due to the decreased distance of electrons to the back contact, the beneficial effect of reducing the back

recombination resulting from the back Ga grading is more pronounced for ultra-thin solar cells than for the typical ones with 2-μm thick absorber. However, the benefit is usually interpreted electrically that an increasing conduction band towards the back contact forms a repelling force, thus preventing the electrons from diffusing towards the back contact. Furthermore, the back Ga grading can also benefit the carrier collection optically for our ultra-thin absorbers. For the higher back [Ga]/[III] profile, more low [Ga]/[III] phases are located away from the back contact and the CIGSe phases near the back contact are higher [Ga]/[III] ratio. Since the absorption ability of CIGSe phases is inversely dependent on the [Ga]/[III] ratio, there exist an inverse grading of absorption ability. This indicates more carriers generating away from the back contact and less near the back contact, thus the carriers are less likely to recombine at the back contact. The schematic diagram is shown in Fig. 5(a).

To further corroborate the analysis, we carried out EQE simulations of CIGSe solar cells by SCAPS 3.2.01 [28]. The configuration of the entire solar cell is AZO/i-ZnO/CdS/CIGS/back contact. To describe the grading of absorption ability on the depth and limit the investigation to the influence of back grading of absorption ability, the absorber is assumed to be made of three sub-absorbers with different [Ga]/[III] ratios and the [Ga]/[III] ratio of the surface sub-absorber was set the same for two different [Ga]/[III] configurations. From the surface to the back contact, the [Ga]/[III]ratio is 0.33, 0.19, 0.48 in sequence for a low back Ga grading and 0.33, 0.0, 0.53 for a high back Ga grading. The corresponding sub-absorbers are 100, 100, 250 nm thick and the overall [Ga]/[III] ratio is thus the same for the two different Ga grading configurations. Absorption coefficient α for each [Ga]/[III]ratio is separately derived from individual layers with according composition. To exclude the electrically beneficial effect of back Ga grading on the carrier collection, the electrical bandgap of each sub-absorber is artificially set to the same value of 1.26 eV for the two [Ga]/[III] profiles. There is no interface defect between the sub-absorbers. To confine the simulation to the optically beneficial effect of back Ga grading, the other parameters of the solar cells are kept the same for both configurations and are reasonable compared to

literature [29, 30] (more details are attached in Appendix 1). SCAPS assumes no reflection between interfaces, thus only a single forward propagating light through every layer is simulated. The forward absorbance (Abs_f) in the absorber was quantitatively calculated by Beer-Lambert law and the external quantum efficiency (EQE_f) was simulated. To describe the collection efficiency of carriers within the absorber, the internal quantum efficiency ($IQE_f = EQE_f/Abs_f$), was deduced and is shown in Fig. 5(b). We can observe that IQE_f has improved much for a high back Ga grading. Additionally, the long-wavelength light can only be absorbed by CIGSe phases with low [Ga]/[III] ratio. This indicates that the corresponding generated carriers are far away from the back contact in our simulation configuration. This is why the IQE_f in the wavelength range of 1050-1200 nm is very high. Conclusively, the high Ga back grading contributes to the collection of carriers optically as well.

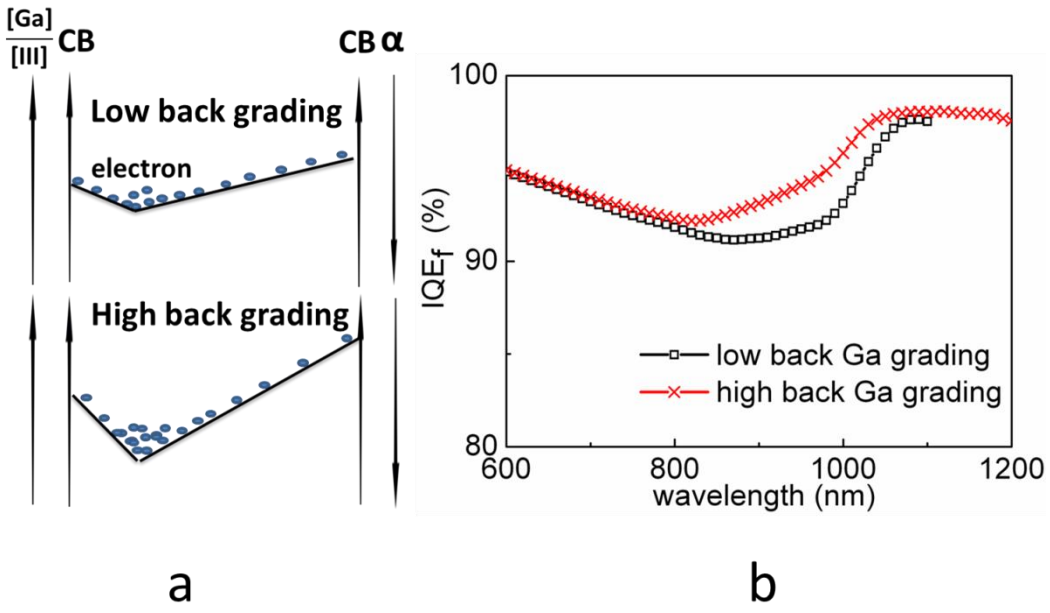

Fig.5: (a) schematic of generation profiles of electrons at both low and high back Ga grading. The conduction band (CB) is directly proportional to the [Ga]/[III] ratio and the absorption coefficient (α) inversely, (b) simulated internal quantum efficiency ($IQE_f = QE_f/Abs_f$) of carriers generated from forward going light within absorbers by SCAPS. The absorber is composed of three sub-absorbers with

corresponding realistic absorption coefficients. The other parameters of solar cell configuration are the same and attached in Appendix 1.

3.3 Implication of low process temperature for light trapping

By lowering the process temperature, J_{SC} is largely enhanced to 26.6 mA/cm^2 in our ultra-thin solar cells. However, J_{SC} is still lower than that from a typical CIGSe solar cell with 2-μm thick absorber (>30 mA/cm^2), which hinders further improvement of the efficiency of ultra-thin solar cells. Decreasing the absorber thickness below 0.5 μm will inevitably lead to incomplete absorption of the incident solar spectrum. Light trapping technologies are therefore essential to realize higher J_{SC} and resulting highly efficient ultra-thin solar cells. The rear light-trapping technologies, like the rear passivation layer with point contacts [12] and back reflector for TCO back contact solar cells [31], can also benefit from the high back Ga grading structure. As we analyzed above in Fig.5, the high back Ga/[III] depth profile is beneficial for the collection of carriers generated from the forward going light. This also works for the backward going light contributing from light trapping technologies. To illustrate this quantitatively, we use the same simulation configuration as in Fig. 5 with further assuming that all unabsorbed light will be 100% normally reflected back at the back contact. There are two passes of light propagating through the absorber: one forward going, one backward going. We simulated the total EQE (EQE_{f+b}) including both forward and backward going light. The EQE_b only contributed from the backward going light is the difference between EQE_{f+b} and EQE_f. Again the absorbance of the backward going light (Abs_b) within the absorber was calculated, the IQE_b from the backward going light ($IQE_b = EQE_b/Abs_b$) was thus deduced and is displayed in Fig. 6. The higher back Ga/[III] profile exhibits higher IQE_b as expected. Besides, the absorption ability of CIGSe is decreasing as the increasing wavelength, so the longer wavelength light can penetrate deeper into the absorber from the back contact. For shorter wavelength light, more carriers will be generated near the back contact and thus the recombination is higher. This explains why the IQE_b increases with the increasing wavelength for the backward going light.

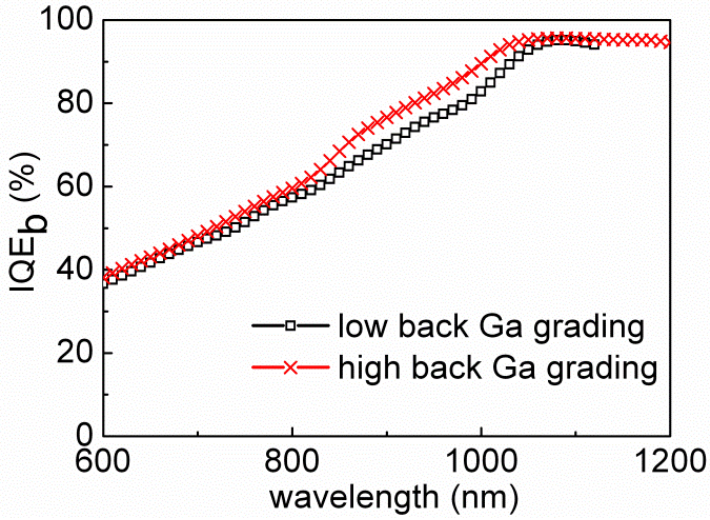

Fig. 6. Simulated internal quantum efficiency ($IQE_b = EQE_b/Abs_b$) of carriers generated from the backward going light

4. Conclusion

Ultra-thin CIGSe solar cells were fabricated by the 3-stage process at two process temperatures of 440 °C and 610 °C. It is discovered that the low process temperature can largely reduce the In-Ga inter-diffusion and create a higher back Ga grading than the high temperature. The higher back Ga grading is beneficial for the solar cells with greatly improved short circuit current density J_{sc} and efficiency η. It is evidenced that a higher Ga grading can enhance the absorption of incident light in terms of a broader absorption spectrum as well as a higher absorption ability above the wavelength of 930 nm. What is more, it is theoretically proved that the high back Ga grading can reduce the back recombination optically as well by shifting the generation of carriers away from the back contact. Finally, it is implied that the high back Ga grading can also improve the collection of the carriers contributed from the back reflected light. As a result, the low process temperature is highly recommended to realize the potential of highly efficient ultra-thin CIGSe solar cells.

Acknowledgements

The authors would like to thank C. Kelch, M. Kirsch, J. Albert and R. Keller for technical support, P. Manley for revising the paper, C.A Kaufmann and R. Klenk for discussing. The authors acknowledge the funding from the Helmholtz-Association for Young Investigator groups within the Initiative and Networking fund (VH-NG-928) and G. Yin specially acknowledges the support of funding from China Scholarship Council.

Appendix :

The collection efficiency of the carriers is simulated by SCAPS. The configuration of the CIGSe solar cell consists of a CIGSe layer (overall thickness d=450 nm), a CdS layer (d=50 nm, bandgap Eg=2.42 eV), an i-ZnO layer (d=130 nm, Eg=3.25 eV), an alumium doped ZnO (AZO) layer (d=240 nm, Eg=3.6 eV). The CIGSe layer is p doped (the effective doping concentration N_A=1.0*E16 /cm^3), the other layers are n doped (N_D=1.0*E14/cm^3 for CdS, 5.0*E17/cm^3 for i-ZnO and 1.0*E20/cm^3 for AZO). To describe the grading of absorption ability on the depth, the absorber is assumed to be made of 3 sub-absorbers with thickenss of 100, 100, 250 nm from surface to back contact. The [Ga]/[III] is 0.33, 0.19, 0.48 in sequence for a low back [Ga]/[III] grading and 0.33, 0.0, 0.53 for a high back [Ga]/[III] grading. The back recombination rate S = 1.0*E07 cm/s, diffusion length of electrons Lp = 250 nm and holes Ln = 570 nm within absorbers. To exclude the electrically beneficial effect of back [Ga]/[III] grading on the carrier collection, the electrical bandgap grading of the high back Ga grading is artificially set flat for both back Ga grading profiles. Absorption coefficient α for each [Ga]/[III]ratio is separately derived from individual layers with according composition. The whole simulation is done by SCAPS 3.2.01 and the complete parameter set can be requested from the author.

References

[1] P. C. K. Vesborg, T. F. Jaramillo, Addressing the terawatt challenge: scalability in the supply of chemical elements for renewable energy, RSC Advances, 2 (2012) 7933–7947.

[2] C. Tao, J. Jiang, M. Tao, Natural Resource Limitations to Terawatt Solar Cell Deployment, ECS Transactions, 33 (2011) 3-11.

[3] O. Lundberg, M. Bodegard, J. Malmstrom, L. Stolt, Influence of the Cu(In,Ga)Se2 thickness and Ga grading on solar cell performance, Prog. Photovolt.: Res. and Appl., 11 (2003) 77-88.

[4] Z. Jehl, F. Erfurth, N. Naghavi, L. Lombez, I. Gerard, M. Bouttemy, P. Tran-Van, A. Etcheberry, G. Voorwinden, B. Dimmler, W. Wischmann, M. Powalla, J.F. Guillemoles, D. Lincot, Thinning of CIGS solar cells: Part II: Cell characterizations, Thin Solid Films, 519 (2011) 7212-7215.

[5] A. Freundlich, N. Naghavi, Z. Jehl, F. Donsanti, J.-F. Guillemoles, I. Gérard, M. Bouttemy, A. Etcheberry, J.-L. Pelouard, S. Collin, C. Colin, N. Péré-Laperne, N. Dahan, J.-J. Greffet, B. Morel, Z. Djebbour, A. Darga, D. Mencaraglia, G. Voorwinden, B. Dimmler, M. Powalla, D. Lincot, J.-F.F. Guillemoles, Toward high efficiency ultra-thin CIGSe based solar cells using light management techniques, in: Proc. of SPIE 8256 (2012) 825617.

[6] M. Gloeckler, J.R. Sites, Potential of submicrometer thickness Cu(In,Ga)Se2 solar cells, J. Appl. Phys, 98 (2005) 103703.

[7] M. Contreras, J. Tuttle, D.H. Du, Y. Qi, A. Swartzlander, A. Tennant, R. Noufi, Graded band-gap Cu(in,Ga)Se2 thin-film solar-cell absorber with enhanced open-circuit voltage, Appl. Phys. Lett., 63 (1993) 1824-1826.

[8] S. Schleussner, U. Zimmermann, T. Wätjen, K. Leifer, M. Edoff, Effect of gallium grading in Cu(In,Ga)Se2 solar-cell absorbers produced by multi-stage coevaporation, Sol. Energy Mater. Sol. Cells, 95 (2011) 721-726.

[9] A.M. Gabor, J.R. Tuttle, M.H. Bode, A. Franz, A.L. Tennant, M.A. Contreras, R. Noufi, D.G. Jensen, A.M. Hermann, Band-gap engineering in Cu(In,Ga)Se2 thin films grown from (In,Ga)2Se3 precursors, Sol. Energy Mater. Sol. Cells, 41-2 (1996) 247-260.

[10] T. Dullweber, G. Hanna, W. Shams-Kolahi, A. Schwartzlander, M.A. Contreras, R. Noufi, H.W. Schock, Study of the effect of gallium grading in Cu(In,Ga)Se2, Thin Solid Films, 361 (2000) 478-481.

[11] M. Troviano, K. Taretto, Temperature-dependent quantum efficiency analysis of graded-gap Cu(In,Ga)Se2 solar cells, Sol. Energy Mater. Sol. Cells, 95 (2011) 3081-3086.

[12]B. Vermang, V.Fjällström, J. Pettersson, P. Salome, M. Edoff, Development of rear surface passivated Cu(In,Ga)Se2 thin film solar cells with nano-sized local rear point contacts, Sol. Energy Mater. Sol. Cells, 117(2013) 505-511.

[13] A.M. Gabor, J.R. Tuttle, D.S. Albin, M.A. Contreras, R. Noufi, A.M. Hermann, High-efficiency CuInxGa1-xSe2 solar-cells made from (InxGa1-x)2Se3 precursor films, Appl. Phys. Lett., 65 (1994) 198-200.

[14] H. Mönig, C.A. Kaufmann, C.H. Fischer, A. Grimm, R. Caballero, B. Johnson, A. Eicke, M.C. Lux-Steiner, I. Lauermann, Gallium gradients in chalcopyrite thin films: Depth profile analyses of films grown at different temperatures, J. Appl. Phys, 110 (2011) 093509.

[15] C.A. Kaufmann, R. Caballero, T. Unold, R. Hesse, R. Klenk, S. Schorr, M. Nichterwitz, H.W. Schock, Depth profiling of Cu(In,Ga)Se2 thin films grown at low temperatures, Sol. Energy Mater. Sol. Cells, 93 (2009) 859-863.

[16]A. Chiril, A. R. Uhl, C. Fella, L. Kranz, J. Perrenoud, S. Seyrling, R. Verma, S. Nishiwaki, Y. E. Romanyuk, G. Bilger, A. N. Tiwaria, S. Buecheler, F. Pianezzi, P.Bloesch, C. Gretener, Highly efficient Cu(In,Ga)Se2 solar cells grown on flexible polymer film, Natural Materials 10 (2011) 857-861.

[17] C.A. Kaufmann, A. Neisser, R. Klenk, R. Scheer, Transfer of Cu(In,Ga)Se2 thin film solar cells to flexible substrates using an in situ process control, Thin Solid Films, 480 (2005) 515-519.

[18] R. Caballero, S. Siebentritt, K. Sakurai 1, C.A. Kaufmann, H.W. Schock, M.Ch. Lux-Steiner, Effect of Cu excess on three-stage CuGaSe2 thin films using in-situ process controls, Thin Solid Films 515(2007) 5862–5866.

[19] R.E. Denton, R.D. Campbell, S.G. Tomlin, The determination of the optical constants of thin films from measurements of reflectance and transmittanceat normal incidence, J. Phys. D: Appl. Phys.,5(1972) 852-863.

[20] D. Abou-Ras, R. Caballero, C.H. Fischer, C.A. Kaufmann, I. Lauermann, R. Mainz, H. Monig, A. Schopke, C. Stephan, C. Streeck, S. Schorr, A. Eicke, M. Dobeli, B. Gade, J. Hinrichs, T. Nunney, H. Dijkstra, V. Hoffmann, D. Klemm, V. Efimova, A. Bergmaier, G. Dollinger, T. Wirth, W. Unger, A.A. Rockett, A. Perez-Rodriguez, J. Alvarez-Garcia,T. Schmid, P.P. Choi, M. Muller, F. Bertram, J. Christen, H. Khatri, R.W. Collins, S. Marsillac, I. Kotschau, Comprehensive comparison of various techniques for the analysis of elemental distributions in thin films, Microsc. Microanal. 17 (2011) 728-751.

[21]V. Efimova, Study in analytical glow discharge spectrometry and its application in materials science, PhD thesis Dresden 2011.

[22] T. Dullweber, U. Rau, M. A. Contreras, R. Noufi, H.W. Schock, Photogeneration and carrier recombination in graded gap Cu(In, Ga)Se Solar Cells, IEEE Trans. Electron Devices, 47 (2000) 2249-2254.

[23] S.S. Hegedus, W.N. Shafarman, Thin-film solar cells: device measurements and analysis, Prog. Photovolt.: Res. and Appl., 12 (2004) 155-176.

[24] A. Niemegeers, M. Burgelman, R. Herberbolz,U.Rau, D. Hariskos, H.-W. Schock, Model for electronic transport in Cu(In,Ga)Se2 Solar cells, Prog. Photovolt.: Res. and Appl., 6 (1998) 407-421.

[25] G. Yin, C. Merschjann, M. Schmid, The effect of surface roughness on the determination of optical constants of CuInSe2 and CuGaSe2 thin films, J. Appl. Phys, 113 (2013).

[26] S. Theodoropoulou, D. Papadimitriou, K. Anestou, C. Cobet, N. Esser, Optical properties of CuIn1−xGaxSe2 quaternary alloys for solar-energy conversion, Semicond. Sci. Technol., 24 (2009) 015014.

[27] K. Orgassa, Coherent optical analysis of the ZnO/CdS/Cu(In,Ga)Se2 thin film solar cell, PhD thesis Stuggart 2004.

[28] M. Burgelman, P. Nollet, S. Degrave, Modelling polycrystalline semiconductor solar cells, Thin Solid Films, 361 (2000) 527-532.

[29] P. Pistor, R. Klenk, On the advantage of a buried pn-junction in chalcopyrite solar cells: An urban legend, In: Proceedings of NUMOS, 2007 179-182

[30] R. Klenk, Characterisation and modelling of chalcopyrite solar cells, Thin Solid Films, 387 (2001) 135-140.

[31] O. Berger, D. Inns, A.G. Aberle, Commercial white paint as back surface reflector for thin-film solar cells, Sol. Energy Mater. Sol. Cells, 91(2007) 1215–1221.